JOURNAL OF THERMOPHYSICS AND HEAT TRANSFER
Vol. 21, No. 2, April–June 2007

Uncertainty Quantification in Estimating Critical Spacecraft Component Temperatures

Daniel P. Thunnissen*
Nanyang Technological University, Singapore 639668, Republic of Singapore
Siu Kui Au†
City University of Hong Kong, Hong Kong, People's Republic of China
and
Glenn T. Tsuyuki‡
Jet Propulsion Laboratory, California Institute of Technology, Pasadena, California 91109

DOI: 10.2514/1.23979

A method for quantifying uncertainty in conceptual-level design via a computationally efficient probabilistic method is presented. The investigated method is applied to estimating the maximum-expected temperature of several critical components on a spacecraft. The variables of the design are first classified and assigned appropriate probability density functions. To characterize the thermal control system of the spacecraft, Subset Simulation, an efficient simulation technique originally developed for reliability analysis of civil engineering structures, is used. The results of Subset Simulation are compared with traditional Monte Carlo simulation. The investigated method allows uncertainty in the maximum-expected temperatures to be quantified based on the risk tolerance of the decision maker. For the spacecraft thermal control problem presented, Subset Simulation successfully replicated Monte Carlo simulation results for estimating the maximum-expected temperatures of several critical components yet required significantly less computational effort, in particular for risk-averse decision makers.

Nomenclature

$B_q(a, b)$	=	incomplete Beta function with parameters a and b
E	=	bus voltage
F	=	failure
G	=	response function
$H(y)$	=	cumulative distribution function of Y
m	=	number of Subset Simulation levels
N	=	number of samples
N_C	=	number of Markov chains developed at each simulation level
N_{SS}	=	number of Subset Simulation samples up to level i
N_T	=	number of Monte Carlo simulation samples
P	=	probability
p	=	failure probability; $\bar{p} + p = 1$
$\bar{p}$	=	confidence level probability
p_0	=	conditional probability for Subset Simulation; $p_0 \in (0, 1)$
Q	=	heat rejected
$\dot{V}$	=	volume flow rate
X	=	general random variable
Y	=	random variable representation of tradable parameter y
Y^t	=	true value of tradable parameter y
y	=	tradable parameter
$y_{\bar{p}}$	=	the "exact" $\bar{p}$-tile value; $P(Y \leq y_{\bar{p}}) = \bar{p}$
α	=	absorptivity
γ	=	correlation factor
δ	=	coefficient of variation
ε	=	emissivity
Θ	=	random variable representation of input parameter θ
θ	=	input variable (parameter)
ξ	=	specified threshold value
ρ	=	correlation coefficient
σ	=	standard deviation of a normal distribution

Subscripts

HRS	=	heat rejection system
HRS_rad	=	heat rejection system radiator
j	=	input variable uncertainty number
REM	=	rover electronics module
SDST	=	small deep space transponder
SSPA	=	solid state power amplifier

Received 17 March 2006; revision received 29 August 2006; accepted for publication 16 September 2006.

*Assistant Professor, School of Mechanical & Aerospace Engineering, 50 Nanyang Avenue. Senior Member AIAA.
†Assistant Professor, Department of Building and Construction, 83 Tat Chee Avenue, Kowloon.
‡Manager, Thermal and Cryogenic Engineering Section, Mail Stop 125-224. Associate Fellow AIAA.

I. Introduction

SPACECRAFT are complex multidisciplinary systems with a dozen or more subsystems. Thermal control is one example of such a spacecraft subsystem (discipline). All complex multidisciplinary systems including spacecraft require engineers and designers to deal with uncertainty. Uncertainty impacts the decisions engineers and managers make in how they design complex multidisciplinary systems. In one extreme, when engineers and managers are risk-tolerant in the context of uncertainty, decisions are made that might ultimately result in systems that are over budget, delivered late, descoped, or even canceled. In the other extreme, when engineers and managers are too risk-averse, uncertainty can lead to decisions that result in uncompetitive, overdesigned systems that are not optimized for the requirements they are designed to satisfy. This impact of uncertainty in thermal control is perhaps best exemplified in the estimation of the operating temperatures of critical spacecraft components. If uncertainty is not properly quantified early in design, an entire subsystem or spacecraft may fail when a critical component reaches a temperature that was not foreseen. Although not as catastrophic but nonetheless costly to the spacecraft manufacturer, an entire subsystem or spacecraft may be overdesigned when anticipated temperatures are predicted and designed around yet never encountered.

Table 1 Examples of different uncertainty types

Uncertainty type	Thermal control example	Included in this paper's analysis?
Ambiguity	The maximum allowable temperature of the battery is 10°C (anywhere? bulk average? etc.)	No
Epistemic		
Model	The difference between the temperature predicted by an analytic model and the actual flight measured temperature	Yes
Phenomenological	Thermal environment on a comet's surface	No
Behavioral		
Design	The choice between two different thermal paints for a spacecraft's exterior	Yes
Requirement	The spacecraft shall be able to reject up to 300 W of heat (and this requirement later changes to 350 W)	Yes
Volitional	An analysis an engineer says he will perform but does not	No
Human errors	A mistake in measuring the area of a thermal radiator	No
Aleatory	Properties, such as emissivity or absorptivity, of a thermal paint	Yes
Interaction	The combination of choice between two different thermal paints and the fact that their properties are not certain	Yes

Uncertainty in complex multidisciplinary systems can be classified into four types: *ambiguity*, *epistemic*, *aleatory*, and *interaction* [1]. Detailed definitions and explanations of these uncertainties as well as an overview of uncertainty taxonomies in a variety of fields are provided in [1]. Table 1 provides examples for each of these uncertainty types in the field of spacecraft thermal control. Because it is arguably more important to determine the significant sources of uncertainty in preliminary design than identifying and quantifying all uncertainty sources, Table 1 also indicates whether this form of uncertainty is viewed as significant and hence, included in the subsequent analysis.

Engineering design can be mathematically formulated as

$$\boldsymbol{y} = \boldsymbol{G}(\boldsymbol{\theta}) \tag{1}$$

Equation (1) represents a general expression for design where a vector $\boldsymbol{\theta}$ of input parameters (variables) is mapped to a vector $\boldsymbol{y}$ of output parameters (tradable parameters) via one or more transformation (response) functions $\boldsymbol{G}$. The response function(s) may be complicated (e.g., closed-form equations, computational algorithms, "black box" functions), requiring significant expense in time and resources to calculate values. Whereas current design methods traditionally assume these input variables are deterministic and uncertainty is evaluated ex-post facto, the method described in this paper follows probabilistic design techniques that quantify the uncertainty in the tradable parameters $\boldsymbol{y}$ by accounting for all the uncertainties in the $\boldsymbol{\theta}$ input variables themselves [2]. In this context, the vector $\boldsymbol{\theta}$ in Eq. (1) is replaced by $\boldsymbol{\Theta}$ that may include discrete random variables, continuous random variables, constant values, and discrete choices among options. The set of output parameters that depend on the random vector $\boldsymbol{\Theta}$ is now denoted by the capital letter $\boldsymbol{Y}$:

$$\boldsymbol{Y} = \boldsymbol{G}(\boldsymbol{\Theta}) \tag{2}$$

Probability theory is well known to provide a rational and consistent framework for treating uncertainties and plausible reasoning [3,4]. Probabilistic methods offer a viable approach to manage uncertainties that confront a decision maker. A decision maker is one or more individuals or organizations responsible for making final decisions in a project. We use the singular in this paper although the decision maker may consist of more than a solitary individual or organization.

The output vector of random variables $\boldsymbol{Y}$ assumes that the given response functions $\boldsymbol{G}$ are "perfect" with no uncertainty in the response functions (models). Approximation error in a given tradable parameter (dependent variable) can be represented as a random variable and related to the true value [2]:

$$Y^t = Y + X \tag{3}$$

A probability density function (PDF) can be determined for X if sufficient data are available to compare to the values determined by the model. Assuming the approximation error X is independent of the model prediction Y, the cumulative distribution function (CDF) of the tradable parameter can be obtained as the convolution of the CDFs of Y and X. A CDF value is selected based on the risk tolerance of the decision maker. The risk tolerance of a decision maker will manifest itself through the particular percentile value, $\bar{p}$, of this CDF the decision maker chooses to believe. For example, the 90, 99, and 99.9 percentiles might provide a decision maker with low-, medium-, and high-confidence estimates in the probability that a tradable parameter will not be exceeded. These three percentiles may correspond to a risk-tolerant, risk-neutral, or risk-averse decision maker, respectively. The extreme tails of a tradable parameter distribution are important in the design of many complex engineering systems. A spacecraft may need an accurate estimate of the 99, 99.9, or 99.99 percentile values for its reliability to see if it will survive long enough to complete its mission, whereas an aircraft would like accurate estimates of the extreme tail values of its range to be certain a target or destination can be reached in an emergency situation. Unfortunately, the traditional method for accessing such uncertainties (Monte Carlo simulation) requires a large number of samples to accurately determine extreme tail (high- or low-percentile) values which may require a prohibitive amount of time and resources to complete. Advanced Monte Carlo methods are being developed with the aim to be applicable to complex engineering systems that involve general nonlinear response and a large number of random variables [5,6]. The method described in this paper applies an innovative sampling technique known as Subset Simulation to accurately determine CDF values of interest while significantly reducing the amount of response function calculations and hence, the total computation cost. Originally developed and applied in estimating small failure probabilities in high-dimension structural-engineering applications, Subset Simulation has been modified to handle more general situations [7–9].

The remainder of the paper summarizes the investigated method, its application to a spacecraft thermal control system, and discusses the results.

II. Method Summary

The general method to evaluate the CDF of Eq. (2) begins with identifying all the tradable parameters of concern to a decision maker. With tradable parameters identified, the engineering system (response function) is formulated mathematically. This mathematical formulation may be an analytic model for each tradable parameter. Such a model might include dozens or hundreds of equations and relations. A model may be existing off-the-shelf software or a custom program for this specific system. Much analysis for spacecraft thermal control is mission-specific and requires customized models. The analysis described in this paper is a combination of the two: a custom thermal model of a specific spacecraft analyzed with an existing off-the-shelf software package. Determining how accurate models need to be to effectively assess uncertainty in conceptual design is a critical issue. In this work,

modeling error is addressed as an additive uncertainty [see Eq. (3)] whose distribution is assigned based on expert judgment.

With models and model uncertainty assessed, the input variables are classified and given a probabilistic representation. Classifying the variables into their uncertainty types is useful in understanding their respective impact on the overall design. Variables are characterized by a PDF. The PDF applied to each variable may be determined from existing data, analogy, analysis, expert opinion, or a combination of these.

To propagate the uncertainty of the input variables and assess the probabilistic characteristics of the tradable parameters, two simulation techniques, Monte Carlo simulation and Subset Simulation, are considered in this work. The former serves as a benchmark for the latter. Uncertainty in the model (approximation error) is assessed at the final step for Monte Carlo simulation. The CDF results for the model response Y obtained by the simulation techniques are probabilistically convolved with the CDF of model uncertainty X to yield final estimate of the uncertainty in each tradable parameter Y' which can then be used by the decision maker to guide design decisions. In Subset Simulation, model uncertainty is treated at the same level as any other uncertainty via an input variable. In this paper, model uncertainty is assumed to be Gaussian with zero mean (implying unbiased prediction) and some appropriate value of variance chosen a priori.

A. Monte Carlo Simulation

Monte Carlo simulation (MCS) is the most established sampling technique and the benchmark for comparison by other techniques. In MCS, N random realizations (samples) of the uncertain input variables, $\boldsymbol{\theta}$, are generated according to their specified probability distributions. The tradable parameters $\boldsymbol{y}$ are then evaluated via the response function(s) $\boldsymbol{G}$ for the generated samples and recorded. The N values for each tradable parameter can be used for estimating the mean or other statistics as well as the PDF and CDF.

Without loss of generality, assume a scalar quantity Y of interest. Using N MCS samples, a simple estimator for the upper $\bar{p}$-percentile value can be obtained as the $\bar{p}N$-th largest value of Y among the N samples, i.e., the $\bar{p}N$-th order statistic, denoted by $Y_{(\bar{p}N)}$. This estimator is asymptotically unbiased and its variance given by

$$\mathrm{var}\,[Y_{(\bar{p}N)}] = \int_0^\infty [y - H^{-1}(pN)]^2 \,\mathrm{d}H_{\bar{p}N}(y) \tag{4}$$

where $H(y)$ is the CDF of Y and $H_{\bar{p}N}(y)$ is the CDF of $Y_{(\bar{p}N)}$ [10]:

$$H_{\bar{p}N}(y) = B_{H(y)}[\bar{p}N, (1-\bar{p})N + 1] \tag{5}$$

and

$$B_q(a,b) = \frac{\int_0^q t^{a-1}(1-t)^{b-1}\,\mathrm{d}t}{\int_0^1 t^{a-1}(1-t)^{b-1}\,\mathrm{d}t} \tag{6}$$

is the incomplete Beta function with parameters a and b. It should be noted that with N samples the highest percentile value that can be estimated corresponds to a confidence level of $\bar{p} = 1 - 1/N$, although such estimator can be significantly biased.

Complementarily, the failure probability $p = P(Y > y)$ for a given y can be estimated simply as the fraction of samples with $Y > y$ among the N MCS samples. The coefficient of variation (COV) of this failure probability estimate is given by

$$\delta = \sqrt{\frac{1-p}{pN}} \sim \frac{1}{\sqrt{pN}} \tag{7}$$

B. Subset Simulation

Subset Simulation (SS) is an adaptive stochastic simulation procedure for efficiently computing small tail probabilities [7,8]. Originally developed for reliability analysis of civil engineering structures, SS stems from the idea that a small failure probability can be expressed as a product of larger conditional failure probabilities for some intermediate failure events, thereby converting a rare event simulation problem into a sequence of more frequent ones. During SS, conditional samples are generated from specially designed Markov chains so that they populate gradually each intermediate failure region until they reach the final target (rare) failure region.

Without loss of generality, assume one tradable parameter Y and that it is positive-valued. For a given ξ for which $P(Y > \xi)$ is of interest, let $0 < \xi_1 < \xi_2 < \ldots < \xi_m = \xi$ be an increasing sequence of intermediate threshold values. By the definition of conditional probability,

$$\begin{aligned} P(Y > \xi) &= P(Y > \xi | Y > \xi_{m-1}) P(Y > \xi_{m-1}) \\ &= \cdots = P(Y > \xi_1) \prod_{i=2}^{m} P(Y > \xi_i | Y > \xi_{i-1}) \end{aligned} \tag{8}$$

The original idea of SS is to estimate $P(Y > \xi_1)$ and $\{P(Y > \xi_1 | Y > \xi_{m-1})\colon i = 2, \ldots, m\}$ by generating samples of $\boldsymbol{\Theta}$ conditional on $\{Y(\boldsymbol{\Theta}) > \xi_i\colon i = 1, \ldots, m\}$. In implementations, the intermediate failure threshold values $\xi_1, \ldots, \xi_m$ are generated adaptively using information from simulated samples so that the sample estimate of $P(Y > \xi_1)$ and $\{P(Y > \xi_i | Y > \xi_{i-1}) :\ i = 2, \ldots, m\}$ always correspond to a common specified value of the conditional probability p_0 (say, $p_0 = 0.1$). By carrying out the procedure until $\xi_m > \xi$, the simulated samples provide information for establishing the CDF of Y covering the small tail probabilities of interest.

1. Markov Chain Monte Carlo

The efficient generation of conditional samples is highly nontrivial but pivotal in the success of SS, and it is made possible through the machinery of Markov Chain Monte Carlo (MCMC) simulation [11]. Markov Chain Monte Carlo is a class of powerful algorithms for generating samples according to any given probability distribution. It originates from the Metropolis algorithm developed by Metropolis et al. for applications in statistical physics [12]. A major generalization of the Metropolis algorithm was due to Hastings for applications in Bayesian statistics [13]. In MCMC, successive samples are generated from a specially designed Markov chain whose limiting stationary distribution tends to the target PDF as the length of the Markov chain increases. Markov chain samples explore and gain information about the failure region as the Markov chain develops.

An essential aspect of the implementation of MCMC is the choice of "proposal distribution" which governs the generation of the next sample from the current one. Such a choice depends on the nature of the input variables and their sensitivity. The efficiency of SS is robust to the choice of the proposal distribution, but tailoring it for a particular class of problem can certainly improve efficiency. Only continuous input variables were considered in the example application and a continuous uniform distribution centered at the current input variable value with a width equal to $2\sigma_j$ is used for the proposal distributions. The computational effort, measured in terms of the number of samples required to achieve a given coefficient of variation for a probability estimate, generally grows in a logarithmic fashion as the target failure probability level p decreases, in contrast to $\mathcal{O}(1/\sqrt{p})$ for traditional Monte Carlo [8].

2. Procedure Overview

The procedure for adaptively generating samples of $\boldsymbol{\Theta}$ conditional on $\{Y(\boldsymbol{\Theta}) > \xi_i\colon i = 1, \ldots, m\}$ corresponding to the target failure probabilities $\{P[Y(\boldsymbol{\Theta}) > \xi_i] = p_0^i,\ i = 1, \ldots, m\}$ by SS is summarized as follows. First, N samples $\{\boldsymbol{\Theta}_{0,k}\colon k = 1, \ldots, N\}$ are simulated by direct Monte Carlo simulation, i.e., they are independent and identically distributed (IID) as the original PDF. The subscript "0" here denotes that the samples correspond to "conditional level 0" (i.e., unconditional). The corresponding values of the tradable variable $\{Y_{0,k}\colon k = 1, \ldots, N\}$ are then computed. The value of ξ_1 is chosen as the $(1 - p_0)N$-th value in the ascending list of $\{Y_{0,k}\colon k = 1, \ldots, N\}$, so that the sample estimate for $P(F_1) = P(Y > \xi_1)$ is always equal to

p_0. Here, we have assumed that p_0 and N are chosen such that p_0N is an integer.

Because of the choice of ξ_1, there are p_0N samples among $\{\Theta_{0,k}: k = 1, \ldots, N\}$ whose response Y lies in $F_1 = \{Y > \xi_1\}$. These are samples at "conditional level 1" and are conditional on F_1. Starting from each of these samples, MCMC is used to simulate an additional $(1 - p_0)N$ conditional samples so that there is a total of N conditional samples at conditional level 1. The value of ξ_2 is then chosen as the $(1 - p_0)N$-th value in the ascending list of $\{Y_{1,k}: k = 1, \ldots, N\}$, and it defines $F_2 = \{Y > \xi_2\}$. Note that the sample estimate for $P(F_2|F_1) = P(Y > \xi_2|Y > \xi_1)$ is automatically equal to p_0. Again, there are p_0N samples lying in F_2. They are samples conditional on F_2 and provide "seeds" for applying MCMC to simulate an additional $(1 - p_0)N$ conditional samples so that there is a total of N conditional samples at "conditional level 2."

This procedure is repeated for higher conditional levels until the samples at "conditional level $(m - 1)$" have been generated to yield ξ_m as the $(1 - p_0)N$-th value in the ascending list of $\{Y_{m-11,k}: k = 1, \ldots, N\}$ and that $\xi_m > \xi$ so that there are enough samples for estimating $P(Y > \xi)$. Note that the total number of samples, i.e., number of evaluations of the tradable variable, required by SS is equal to $N + (m - 1)(1 - p_0)N$. This procedure is illustrated in Fig. 1.

The response values in SS corresponding to tail probabilities (e.g., 1%, 0.1%) yield estimates for the $(1 - p)$ percentile values (e.g., 99%, 99.9%). Thus, the confidence level probability $\bar{p}$ in percentile estimation and the failure probability p in reliability analysis are complementary, i.e., $\bar{p} + p = 1$. Subset Simulation does not explicitly have a fixed failure region but creates intermediate failure regions that have relatively large conditional failure probabilities. The SS formulation is thus appealing in determining tradable parameter uncertainties that do not have fixed failure regions per se. Although SS assumes that the tail of the distribution of interest to a decision maker is the high-percentile end (i.e., 99%, 99.9%), it can also handle the low-percentile end (i.e., 1%, 0.1%) by recasting the problem. In either case, SS can efficiently explore either end of a distribution of interest.

3. *Estimation Error*

Approximate formulae have been derived to assess the error in the failure probability estimates [8], although no formula has been obtained for the statistical error in the percentile estimates. The coefficient of variation δ of the estimate for $P(Y > \xi_m)$, defined as the ratio of its standard deviation to its mean, may be bounded above by using

$$\delta^2 \leq \sum_{i,j=1}^{m} \delta_i \delta_j + \mathcal{O}(1/N) \tag{9}$$

where δ_i is the COV of the estimate for $P(Y > \xi_i|Y > \xi_{i-1})$, with the convention that $P(Y > \xi_1|Y > \xi_0) = P(Y > \xi_1)$, given by

$$\delta_i^2 = \frac{1 - p_0}{p_0 N}(1 + \gamma_i) \tag{10}$$

In Eq. (10), γ_i is a correlation factor that reflects the correlation among the samples at the $(i - 1)$-th conditional level and is given by

$$\gamma_i = 2 \sum_{k=1}^{N/N_c - 1} \left(1 - \frac{kN_c}{N}\right) \rho_i(k) \tag{11}$$

where $N_c = p_0N$ is the number of Markov chains developed at each simulation level (p_0 is assumed to be chosen such that p_0N is an integer), $\rho_i(k)$ is the correlation coefficient evaluated at k Markov chain samples apart at the i-th simulation level, and $\rho_i(k)$ can be estimated using the simulated samples. Note that $\gamma_1 = 0$ as the initial simulation stage correspond to a traditional Monte Carlo simulation. The value of γ_i for $i = 2, \ldots, m$ can be estimated using the Markov chain samples at each $(i - 1)$-th conditional level.

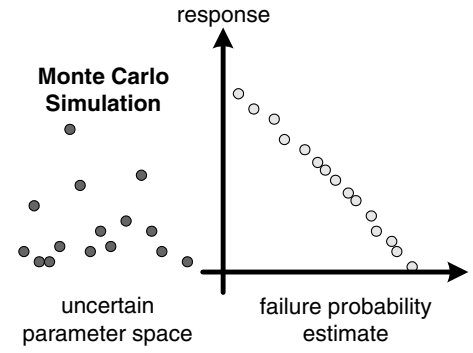

a) Level 0 (initial phase): Monte Carlo simulation

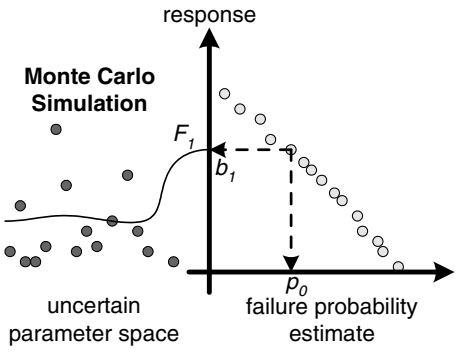

b) Level 0: adaptive selection of first intermediate threshold level

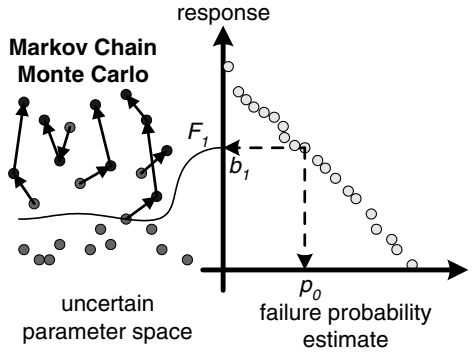

c) Level 1: Markov Chain Monte Carlo simulation

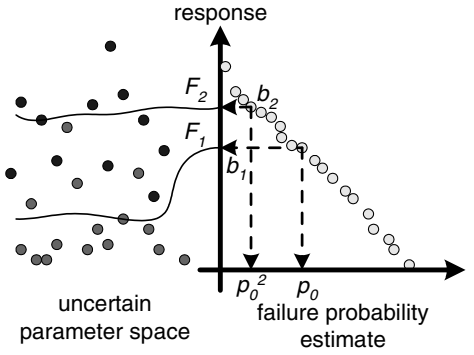

d) Level 1: adaptive selection of second intermediate threshold level

Fig. 1 Illustration of Subset Simulation procedure.

Because from Eq. (10), δ_i is $\mathcal{O}(1/\sqrt{N})$, Eq. (9) indicates that the COV δ of the failure probability estimate is $\mathcal{O}(1/\sqrt{N})$, which is similar to standard Monte Carlo simulation. The actual value of δ depends on the correlation between the intermediate conditional probability estimates, which arises from the fact that some of the samples from one simulation level are used for generating the samples of the next level. The upper bound in Eq. (9) corresponds to the case when the conditional probability estimates are fully correlated. At the other extreme, if all the intermediate conditional probabilities were uncorrelated, then

$$\delta^2 = \sum_{i=1}^{m} \delta_i^2 \tag{12}$$

Experience shows that when the proposal distribution is properly chosen, δ is more closely approximated by Eq. (12) than by the upper bound in Eq. (9).

III. Application

The investigated method is applied to estimating the maximum-expected temperature of four critical components on a spacecraft, specifically the Jet Propulsion Laboratory (JPL)/NASA Mars Exploration Rover (MER) cruise stage. The analysis that follows was performed ex-post facto at an assumed period just before the preliminary design review (PDR). Preliminary design review is one of the most important periods for determining and updating uncertainty estimates in the development of a spacecraft. Although not performed in this paper, the method can be repeated at other times during design to further update uncertainty estimates. For simplicity, only four critical components, namely, the solid state power amplifier (SSPA), rover electronics module (REM), small deep space transponder (SDST), and battery, are investigated. The results of this method are compared to the actual maximum-recorded temperature values obtained from flight data.

A. Mars Exploration Rover Spacecraft

The MER project had the primary objective of placing two mobile science laboratories, MER-A (Spirit) and MER-B (Opportunity), on the surface of Mars to remotely conduct geologic investigations, including characterization of a diversity of rocks and soils that may hold clues to past water activity. The MER project used the 2003 launch opportunity to deliver two identical rovers to different sites in the equatorial region of Mars. The MER project was managed by JPL, a federally funded research and development facility managed by the California Institute of Technology for NASA. The design of MER officially began in April 2000. The MER flight system was an adaptation of the Mars Pathfinder (MPF) spacecraft design which was launched in 1996 and landed successfully on Mars on 4 July 1997. The MER flight system comprised four major components: an Earth–Mars cruise stage; an entry, descent, and landing system; a lander; and a mobile science rover with an integrated instrument package. Figure 2 illustrates the MER flight system. During this interplanetary transfer from Earth to Mars, MER was a spin-stabilized spacecraft with a nominal spin rate of 2 rpm and the cruise stage provided most of the traditional spacecraft subsystem functionality, such as propulsion, power, communications, thermal, and attitude control [14]. Roncoli and Ludwinski [14] discuss the MER mission in detail.

B. Major Assumptions and Model Formulation

The temperatures of components throughout the spacecraft are determined using the network-style thermal simulator SINDA/FLUINT (version 4.6) distributed by Cullimore and Ring Technologies, Inc. (Littleton, Colorado). Originally developed in the 1960s, SINDA (System Improved Numerical Differencing Analyzer) is now used by over 400 sites in the aerospace, energy, electronics, automotive, aircraft, and petrochemical industries for design, simulation, and optimization of systems involving heat transfer and fluid flow [15]. The SINDA software determines the temperature of all components on the spacecraft via nodes. The analytical model for the Mars Exploration Rover cruise stage was intended to serve as a design tool for the employed passive and active thermal control approaches. The use of thermal insulation and thermostatically controlled heaters comprised the majority of the passive techniques. On the other hand, the mechanically pumped fluid loop that transferred waste heat from the Rover and some cruise stage equipment and rejected this heat from radiators on the cruise stage represented the cornerstone of the active thermal control approach. These elements were explicitly modeled. Other thermally significant interactions such as the cruise solar array power shunting due to array switching and the propulsion system thermal maintenance were also captured.

In total, the model was composed of 907 lumped nodes (492 diffusion, 414 arithmetic, and 1 boundary) and 29,356 conductors. The model format was consistent with the commercially available SINDA/FLUINT code. This SINDA model was based on a previous MPF model and was adapted to the MER mission. The MER SINDA model includes a submodel for the heat reduction system (HRS) fluid loop. The internodal radiation interchange conductors and environmental heating were determined through Monte Carlo ray tracing. Simulations could be performed for steady-state or transient conditions. For estimating the maximum-expected component temperatures, the worst-case hot analysis was investigated which occurs in the vicinity of Earth at 1.01 astronomical units and an off-sun angle of 60 deg.

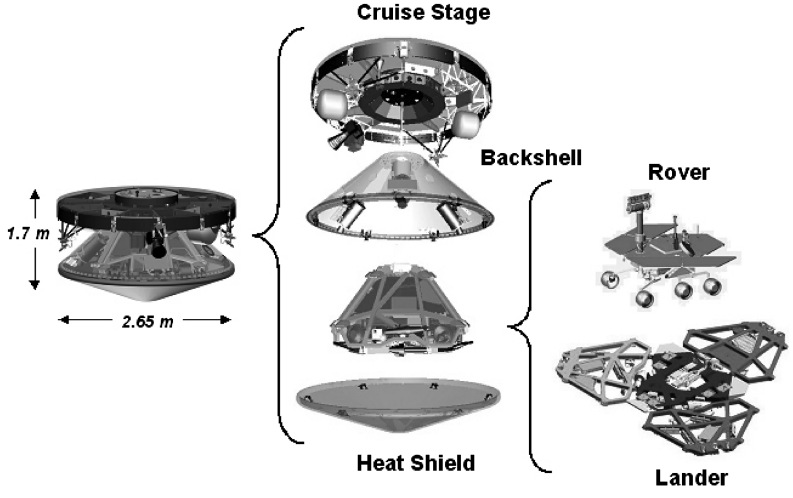

Fig. 2 MER flight system configuration.

Table 2 Uncertain input variables

Variable	Description	Type	Distribution type and parameters
E	Bus voltage, V	Aleatory	Triangular PDF from 27 to 32 with a peak at 30
$\dot{V}_{\mathrm{HRS}}$	Volume flow rate of the heat rejection system, mL/s	Design	Triangular PDF from 8.8 to 12.6 with a peak at 10.1
Q_{REM}	Heat rejected from the rover electronics module, W	Requirement	Uniform PDF from 32 to 37
Q_{SDST}	Heat rejected from the small deep space transponder, W	Requirement	Uniform PDF from 13.7 to 15.1
Q_{SSPA}	Heat rejected from the solid state power amplifier, W	Requirement	Uniform PDF from 32 to 45
$\alpha_{\mathrm{HRS_{rad}}}$	Absorptivity of the heat rejection system	Aleatory	Uniform PDF from 0.17 to 0.35
$\varepsilon_{\mathrm{HRS_{rad}}}$	Emissivity of the heat rejection system	Aleatory	Uniform PDF from 0.80 to 0.91

Because tracking ~900 temperatures and documenting the results within the framework presented is prohibitive, the temperatures of only the SSPA, REM, SDST, and rover battery were explicitly tracked in this analysis. These four components were critical components for the success of the MER mission. Specifically, the MER project wanted to be certain what the highest temperatures these components would attain and design the rest of the system accordingly. The maximum-expected temperatures of the SSPA, REM, SDST, and rover battery were estimated to be 50, 50, 50, and 10°C, respectively, using a worst-case deterministic approach [16]. The MER project also wanted to know the coldest temperatures these components would experience. However, this situation would not occur during cruise, but instead on the surface of Mars, and was not included in this analysis.

C. Classification and Probabilistic Modeling of Variables

The SINDA model contains 384 explicit input variables (such as individual component heat dissipations and global control variables) and another 28,029 implicit input variables (such as external radiation conductors, optical properties, and thermal blanket effective emittance). Seven of the more important/uncertain input variables are assumed uncertain quantities and classified either as aleatory, design, or requirement uncertainties. The remaining variables are assumed certain (constant). The classification aids in understanding the impact of uncertainty in the design and development of the thermal control system. Table 2 lists these uncertainties and their representation in the analysis. For each variable, the probability distribution assumed and the corresponding parameters that define that probability distribution are provided. The various distributions listed in Table 2 were determined primarily by expert opinion (MER engineers and managers) assuming MER was in the conceptual design phase, just before PDR. It should be noted that techniques are available to evaluate the impact of all variables (if desired) but such techniques do not provide full information because of their approximate and perturbation nature.

D. Model Uncertainty

The SINDA model itself is also uncertain. Model uncertainty was briefly discussed in the Introduction and is discussed in detail in [9]. All models are unavoidably simplifications of the reality. They may be compared with a statistically significant number of real phenomena or products and a probabilistic distribution can be constructed to represent this type of uncertainty. This model uncertainty distribution can then combined with the PDF resulting from the Monte Carlo simulation. In the case of SINDA predicted temperatures, it was assumed that its model uncertainty could be represented by a normal distribution with a mean of 0°C and a standard deviation of 2.5°C. That is to say, SINDA correctly predicts 95% of temperatures within five degrees of flight values. This distribution for model uncertainty was determined from expert opinion. A more rigorous distribution, based on actual SINDA, test, and flight data is preferable but was not completed. Such an analysis has been performed for two passive spacecraft thermal control systems [17]. Unfortunately, the PDFs (histograms) presented in [17] cannot be used because the MER thermal control system is active due to the pumped fluid loop and significantly different in overall design and requirements.

E. Simulation and Analysis of Results

Subset Simulation is currently coded in MATLAB® with a graphical user interface that provides a flexible environment for specifying the probability distribution of parameters. As with many general purpose stochastic analysis software [18], an interface has to be built with an external analysis software (in the current study, SINDA/FLUINT) to implement the simulation process in an automated manner. A deterministic case with input variables assuming their nominal values was first run to compare with subsequent probabilistic results. The results of this deterministic case indicated the maximum-expected operating temperature of the SSPA, REM, SDST, and battery to be 27.8, 17.0, 16.7, and 16.7°C. For the two simulation techniques, the number of calls to the SINDA model was set at $N_T = 10,000$ for MCS. Subset Simulation is implemented with $p_0 = 0.1$. Four conditional simulation levels (0 to 3), each with $N = 100$ samples, are carried out so that the smallest tail probability that can be covered is of the order of 10^{-4}. In other words, the total number of calls to SINDA model is $100 + 3 \times 90 = 370$ per run, and confidence limits up to 99.99% are covered. An additional SS run was completed with $N = 500$ samples for the SSPA only to compare with the SS results using 100 samples.

The CDF values of the maximum-expected temperature of the SSPA for both MCS and SS are shown in Figs. 3–6. These figures reflect the final uncertainty in the maximum-expected temperature where model uncertainty has been accounted for. Monte Carlo simulation is the benchmark for comparison but requires a substantial number of calls ($N_T = 10,000$) to the model to obtain values for the entire CDF range. As theorized, SS provides a comparable accuracy as MCS at the CDF tail yet requires substantially less calls to the model. The results of SS for 500 samples are slightly better vis-à-vis 100 samples, although the improved accuracy may not warrant the 1850 total calls to the model that are required.

Table 3 details the statistics of SS by simulation level for the SSPA for 100 samples. The first row of data shows the number of samples used in a single run of SS performed up to different conditional levels (0 to 3). The percentile estimates are shown in the fourth row, where

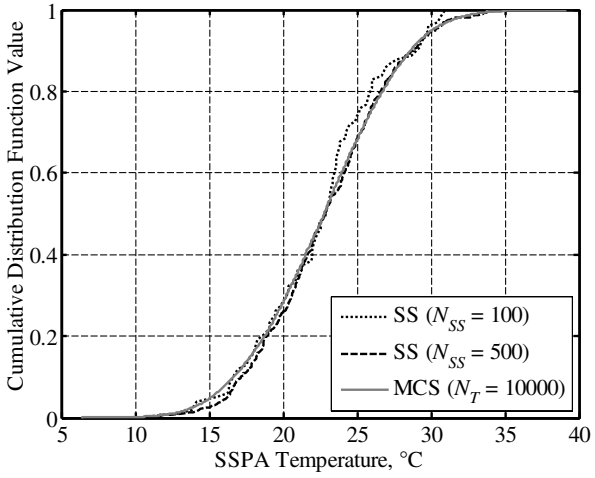

Fig. 3 Maximum-expecting SSPA temperature CDFs (simulation level 0).

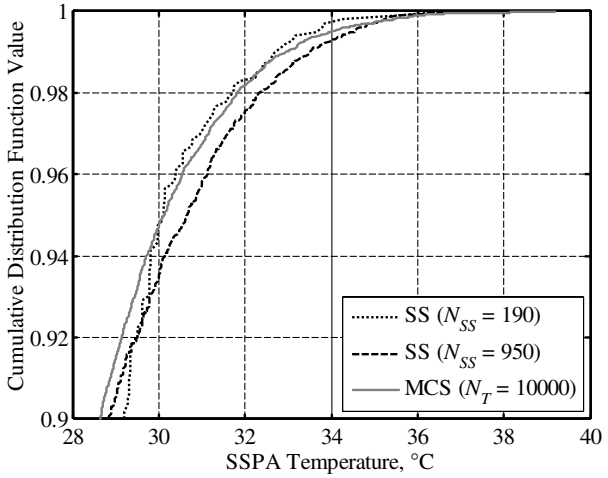

Fig. 4 Maximum-expecting SSPA temperature CDFs (simulation level 1).

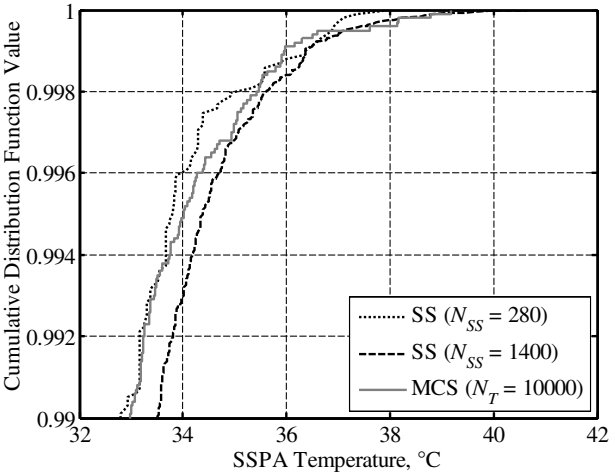

Fig. 5 Maximum-expecting SSPA temperature CDFs (simulation level 2).

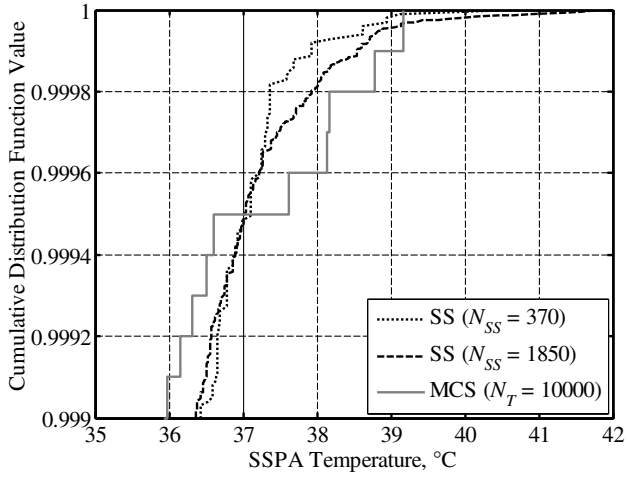

Fig. 6 Maximum-expecting SSPA temperature CDFs (simulation level 3).

number in parentheses shows the associated COV estimated based on 50 independent runs. For each conditional level, the percentile estimates obtained by MCS using the same number of samples N_{SS} are shown in the fifth row. It can be seen that with the same number of samples, SS and MCS yield similar accuracy in the percentile estimates for conditional levels 0 and 1. For higher conditional levels, SS continues to yield percentile estimates with a reasonable accuracy but MCS fails to give higher percentile estimates because by means of order statistic it can only give estimates for $\bar{p} \leq 1 - 1/N$. To provide percentile estimates using MCS, at least 1000 and 10,000 samples are required for $\bar{p} = 99.9\%$ (level 2) and $\bar{p} = 99.99\%$ (level 3), respectively.

The sixth row of data in Table 3 shows the COV of SS estimate for the failure probability $P(Y > y_{\bar{p}})$ at fixed percentile thresholds $y_{\bar{p}}$ given by the MCS benchmark values (third row). The COVs for conditional levels 2 and 3 are unacceptable but they can always be reduced by increasing N (and hence N_{SS}); e.g., doubling the value of N from 100 to 200 will lead to a $1 - 1/\sqrt{2} \approx 30\%$ reduction in the COV's. Nevertheless the corresponding COV's in the percentile estimates (fourth row) are well within tolerance. This indicates that with the same accuracy requirement in COV, it is computationally more demanding to estimate tail probabilities $P(Y > y_{\bar{p}})$ (for a given $y_{\bar{p}}$) than to estimate the percentiles $y_{\bar{p}}$ (for a given $\bar{p}$). This is essentially due to the fact that the failure probability is more sensitive to $y_{\bar{p}}$ than is the percentile to $\bar{p}$. Which quantity to estimate in applications depends on the specific purpose of analysis.

The seventh row in Table 3 shows the equivalent number of MCS samples to achieve the same accuracy in the SS estimates. It is clear that as the conditional level increases, SS becomes computationally more efficient. In particular, at conditional level 3, it requires only a tenth the computational effort of MCS.

The actual maximum temperature of the SSPA was determined from flight data to be 32.5°C, indicating that both MCS and SS provide a much more realistic bound than the worst-case deterministic approach, which estimated the maximum SSPA temperature to reach 50°C [16]. Indeed, 32.5°C corresponds to approximately the 98th percentile value, which illustrates the importance in the risk tolerance of the decision maker in choosing an appropriate CDF value to assume. A risk-tolerant decision maker may have chosen a 90th percentile value (28.8°C), which would have resulted in temperatures being exceeded. In this case a risk-neutral or risk-averse CDF value is appropriate as their corresponding CDF

Table 3 SS results by level for the SSPA ($N = 100$)

	Subset Simulation conditional level i			
	0	1	2	3
N_{SS}	100	190	280	370
$\bar{p}$	90%	99%	99.9%	99.99%
$y_{\bar{p}}$, °C (MCS, single run with 10,000 samples)	28.65	32.97%	35.96%	38.98%
SS single-run estimate for $\bar{p}$-tile (δ),[a] °C	29.20 (2.3%)	32.80 (2.7%)	36.43 (2.6%)	37.92 (2.9%)
MCS single-run estimate for $\bar{p}$-tile using N_{SS} samples (δ),[b] °C	29.04 (2.5%)	31.67 (3.2%)	—— (——)[c]	—— (——)[c]
δ of SS estimate for $P(Y > y_{\bar{p}})$[d]	26%	54%	96%	164%
Equivalent number of MCS samples to achieve the same δ in failure probability[e]	131	345	1080	3723

[a]COV value shown in parentheses, estimated using 50 independent runs.
[b]Estimated as the $\overline{p}N_{SS}$-th order statistic, COV shown in parentheses, estimated based on Eq. (4).
[c]Percentile value cannot be estimated using order statistic because $\bar{p} > 1 - 1/N_{SS}$.
[d]COV estimated using 50 independent runs.
[e]Based on $N_T = \bar{p}/(1 - \bar{p})\delta^2$.

Table 4 SS results by level for the REM ($N = 100$)

	Subset Simulation conditional level i			
	0	1	2	3
N_{SS}	100	190	280	370
$\bar{p}$	90%	99%	99.9%	99.99%
$y_{\bar{p}}$, °C (MCS, single run with 10,000 samples)	18.55	22.55	25.56	28.08
SS single-run estimate for $\bar{p}$-tile (δ),[a] °C	19.08 (3.8%)	23.37 (4.4%)	24.94 (4.3%)	26.82 (4.0%)
MCS single-run estimate for $\bar{p}$-tile using N_{SS} samples (δ),[b] °C	18.10 (3.7%)	21.53 (4.5%)	—— (——)[c]	—— (——)[c]
δ of SS estimate for $P(Y > y_{\bar{p}})$[d]	29%	61%	116%	176%
Equivalent number of MCS samples to achieve the same δ in failure probability[e]	110	270	738	3213

[a]COV value shown in parentheses, estimated using 50 independent runs.
[b]Estimated as the $\bar{p}N_{SS}$-th order statistic, COV shown in parentheses, estimated based on Eq. (4).
[c]Percentile value cannot be estimated using order statistic because $\bar{p} > 1 - 1/N_{SS}$.
[d]COV estimated using 50 independent runs.
[e]Based on $N_T = \bar{p}/(1 - \bar{p})\delta^2$.

Table 5 SS results by level for the SDST ($N = 100$)

	Subset Simulation conditional level i			
	0	1	2	3
N_{SS}	100	190	280	370
$\bar{p}$	90%	99%	99.9%	99.99%
$y_{\bar{p}}$, °C (MCS, single run with 10,000 samples)	18.39	22.42	25.48	27.83
SS single-run estimate for $\bar{p}$-tile (δ),[a] °C	17.69 (3.7%)	22.95 (4.4%)	24.73 (4.0%)	26.11 (4.0%)
MCS single-run estimate for $\bar{p}$-tile using N_{SS} samples (δ),[b] °C	18.65 (3.7%)	21.27 (4.6%)	—— (——)[c]	—— (——)[c]
δ of SS estimate for $P(Y > y_{\bar{p}})$[d]	26%	59%	134%	158%
Equivalent number of MCS samples to achieve the same δ in failure probability[e]	149	302	536	4314

[a]COV value shown in parentheses, estimated using 50 independent runs.
[b]Estimated as the $\bar{p}N_{SS}$-th order statistic, COV shown in parentheses, estimated based on Eq. (4).
[c]Percentile value cannot be estimated using order statistic because $\bar{p} > 1 - 1/N_{SS}$.
[d]COV estimated using 50 independent runs.
[e]Based on $N_T = \bar{p}/(1 - \bar{p})\delta^2$.

Table 6 SS results by level for the battery ($N = 100$)

	Subset Simulation conditional level i			
	0	1	2	3
N_{SS}	100	190	280	370
$\bar{p}$	90%	99%	99.9%	99.99%
$y_{\bar{p}}$, °C (MCS, single run with 10,000 samples)	18.89	22.32	25.31	27.04
SS single-run estimate for $\bar{p}$-tile (δ),[a] °C	19.48 (3.2%)	23.50 (3.0%)	26.24 (3.5%)	27.16 (4.0%)
MCS single-run estimate for $\bar{p}$-tile using N_{SS} samples (δ),[b] °C	18.92 (3.2%)	21.15 (3.9%)	—— (——)[c]	—— (——)[c]
δ of SS estimate for $P(Y > y_{\bar{p}})$[d]	26%	54%	97%	116%
Equivalent number of MCS samples to achieve the same δ in failure probability[e]	130	342	1063	7406

[a]COV value shown in parentheses, estimated using 50 independent runs.
[b]Estimated as the $\bar{p}N_{SS}$-th order statistic, COV shown in parentheses estimated based on Eq. (4).
[c]Percentile value cannot be estimated using order statistic because $\bar{p} > 1 - 1/N_{SS}$.
[d]COV estimated using 50 independent runs.
[e]Based on $N_T = \bar{p}/(1 - \bar{p})\delta^2$.

values would encompass the actual maximum flight temperature recorded.

Finally, Tables 4–6 detail the statistics of SS by simulation level for the REM, SDST, and battery, respectively. Similar efficiency as before is observed for SS.

IV. Conclusions

A method for quantifying uncertainty in conceptual-level design via Subset Simulation is described. As an example application, the investigated method is applied to estimating the maximum-expected temperature of several critical components on the Mars Exploration Rover spacecraft. The results of Subset Simulation are compared with traditional Monte Carlo simulation. The investigated method allows uncertainty in the maximum temperature of critical spacecraft components to be quantified based on the risk tolerance of the decision maker. For the thermal control example presented, Subset Simulation successfully replicated Monte Carlo simulation results for estimating the maximum-expected temperatures of several critical components yet required significantly less computational effort, especially for extremely risk-averse decision makers.

Acknowledgments

This research is funded in part by the Singapore Ministry of Education through research grant ARC8/05. The MER thermal design effort was carried out by the Jet Propulsion Laboratory, California Institute of Technology under a contract with the National Aeronautics and Space Administration. The authors thank Robert Krylo, Eric Sunada, Gani Ganapathi, Gaj Birur (Thermal and Cryogenic Engineering Section, Jet Propulsion Laboratory, Pasadena, California); Brent Cullimore (C&R Technologies, Inc., Littleton, Colorado); and John Welch (The Aerospace Corporation, El Segundo, California) for their consultation and expertise.

References

[1] Thunnissen, D., "Uncertainty Classification for the Design and Development of Complex Systems," *Proceedings of the 3rd Annual Predictive Methods Conference*, Veros Software, Santa Ana, CA, June 2003.

[2] Siddall, J., *Probabilistic Engineering Design: Principles and Applications*, Marcel Dekker, New York, 1983.

[3] Papoulis, A., *Probability, Random Variables, and Stochastic Processes*, McGraw–Hill, New York, 1965.

[4] Jaynes, E., and Jaynes, E. T., *Papers on Probability, Statistics, and Statistical Physics*, Kluwer Academic Publishers, Dordrecht, Holland, 1989.

[5] Pradlwarter, H. J., Pellissetti, M. F., Schenk, C. A., Schueller, G. I., Kreis, A., Fransen, S., Calvi, A., and Klein, M., "Realistic and Efficient Reliability Estimation for Aerospace Structures," *Computer Methods in Applied Mechanics and Engineering*, Vol. 194, Nos. 12–16, April 2005, pp. 1597–1617.

[6] Pellissetti, M. F., Schueller, G. I., Pradlwarter, H. J., Calvi, A., Fransen, S., and Klein, M. "Reliability Analysis of Spacecraft Structures Under Static and Dynamic Loading," *Computers and Structures*, Vol. 84, No. 21, Aug. 2006, pp. 1313–1325.

[7] Au, S. K., "On the Solution of First Excursion Problems by Simulation with Applications to Probabilistic Seismic Performance Assessment," Ph.D. Thesis, California Institute of Technology, Pasadena, CA, 2001.

[8] Au, S. K., and Beck, J., "Estimation of Small Failure Probabilities in High Dimensions by Subset Simulation," *Probabilistic Engineering Mechanics*, Vol. 16, No. 4, 2001, pp. 263–277.

[9] Thunnissen, D., "Propagating and Mitigating Uncertainty in the Design of Complex Multidisciplinary Systems," Ph.D. Thesis, California Institute of Technology, Pasadena, CA, 2005.

[10] David, H. A., *Order Statistics*, John Wiley & Sons, New York, 1981.

[11] Roberts, C., and Casella, G., *Monte Carlo Statistical Methods*, Springer, New York, 1999.

[12] Metropolis, N., Rosenbluth, A., Rosenbluth, M., and Teller, A., "Equations of State Calculations by Fast Computing Machines," *Journal of Chemical Physics*, Vol. 21, No. 6, 1953, pp. 1087–1092.

[13] Hastings, W., "Monte Carlo Sampling Methods Using Markov Chains and Their Applications," *Biometrika*, Vol. 57, No. 1, 1970, pp. 97–109.

[14] Roncoli, R., and Ludwinski, J., "Mission Design Overview for the Mars Exploration Rover Mission," AIAA Paper 2002-4823, Aug. 2002.

[15] Cullimore, B., Ring, S., and Johnson, D., *SINDA/FLUINT User's Manual*, Revision 17, C&R Technologies, Inc., Littleton, CO, Sept. 2003.

[16] Thunnissen, D., and Tsuyuki, G., "Margin Determination in the Design and Development of a Thermal Control System," *SAE 2004 Transactions: Journal of Aerospace*, Vol. 113-1, Society of Automotive Engineers, Warrendale, PA, 2005, pp. 899–916.

[17] Welch, J., "A Comparison of Satellite Flight Temperatures with Thermal Balance Test Data," SAE Technical Paper 2003-01-2460, July 2003.

[18] Schueller, G. I. (ed.), "Special Issue on General-Purpose Software for Structural Reliability Analysis," *Structural Safety*, Vol. 28, Nos. 1–2, 2006.